Bol. Soc. Paran. Mat.
©SPM – E-ISSN-2175-1188
SPM: www.spm.uem.br/bspm

(3s.) **v. 2026 (44)** : 1–12.
ISSN-0037-8712
doi:10.5269/bspm.79535

A Finite Element Approach for Bubble Formation During Laser-Induced Thermotherapy (LIT) of Breast Cancer Tumor

Asif Nawaz, Ghulam Saddiq, Ahmad Saeed, Rozalina Binti Zakaria, N. A. Mardhiah Zainuddin and Saeed Ul Islam

ABSTRACT: Laser induced interstitial thermotherapy LITT is a minimally invasive process intended for precise aiming at breast cancer tumors. Based on the principle of controlled and localized heat ablation. We developed a theoretical computational model emphasizes the role and importance of water present within the tissue. During LITT, vaporization of water taken into account to encounter energy changes. A finite element method was used to probe, the effects of vaporization and development of froths using a bubble formation model. We investigated bubble formation and vaporization by studying the effects of laser power, bubble size and radius effects. The generated results demonstrated tissue water density variations relative to heat influx and pertaining to both tissue heat evolution and its reaction to vaporization processes.

Keywords: Laser induced interstitial thermotherapy (LITT), breast cancer, vaporization, finite element model.

Contents

1. Introduction

The World Health Organization (WHO) lists cancer as the second foremost reason of mortality throughout Europe. The European population represents one eighth of global numbers, yet it has approximately a quarter of all cancer patient cases during a yearly period with 3.7 million new cases occurring. Cancer causes the passing of 1.8 million European each year. Weekly consumption of tobacco combined with alcohol in excess results in 40% of entire cancer cases. Breast cancer and lung cancer exhibit the most dangerous cancer-related mortality. Breast cancer is often influenced by hormonal, genetic, and reproductive determinants [1,2], whereas lung cancer is predominantly associated with environmental exposures such as tobacco use and air pollution [3,4]. Despite these differences, both conditions demonstrate significantly improved treatment outcomes when diagnosed at an early stage, underscoring the critical importance of timely detection and intervention [5,6]. Cancer treatment has an excellent rate of success for multiple tumor types when detection occurs during early stages. Medical professionals consider tumor removal surgery as the primary therapy and its successful recovery potential remains substantial. A hepatic tumor resection remains possible for only 20–25% of patients who have this condition [7]. Breast cancer exists as the top cancer diagnosis among women who receive new cancer diagnoses each year with primary status as the second leading cause of cancer-related fatalities worldwide among female patients. The diagnosis of breast cancer requires physical examination in combination with breast imaging techniques and tissue biopsy. In many Western populations, breast cancer is often detected

2020 *Mathematics Subject Classification:* 92C50.
Submitted October 14, 2025. Published March 22, 2026

through routine health screenings, even before noticeable symptoms appear. The identification of breast cancer normally occurs through physical touch of palpable breast masses before screening tests become available. Medical treatment of breast cancer includes surgery with radiation therapies and chemotherapy while immunotherapy may be employed according to stages and tumor types. [8]. Laser Induced Interstitial Thermal Therapy (LITT) is an encouraging breakthrough in breast cancer therapy with a less invasive approach than the conventional therapies. Unlike traditional approaches that often result in significant tissue damage, long recovery periods, and systemic side effects, LITT allows for precise, localized destruction of tumor cells using controlled thermal energy delivered via laser. This technique not only minimizes harm to surrounding healthy tissue, reduces treatment-related pain and brings about better cosmetic results along with reduced hospital stay durations. As research into breast-conserving therapies advances, LITT emerges as a valuable tool in the pursuit of safer, more effective, and patient-friendly cancer treatments [9].

Thermal ablation functions as an alternative therapy choice following surgery denial because it utilizes temperatures to destroy cancer tissue. Thermal ablation serves as an interventional procedure to treats liver, breast and brain cancer tumors. Cancer cells require complete destruction for preventing their return. When performing surgery, one should protect essential healthy tissues from damage as much as possible. The need for imaging becomes clear due to this situation. Microwave Ablation (MW), Laser-induced Thermotherapy (LITT) and Radiofrequency Ablation (RF) are now combined with Cryotherapy as methods for cancer thermal treatments [10].

This paper describes the modeling of bubbles which occur during LITT of breast cancer tumor treatment. Accurate detection and localization of breast tumors are foundational to the success of Laser-Induced Interstitial Thermal Therapy. Prior to initiation of LITT, tumors are typically identified using imaging modalities, such as magnetic resonance imaging (MRI), ultrasonography and mammography. These techniques not only confirm the presence of malignancy, but also provide high-resolution spatial data that guides the laser fibers placement for precise thermal ablation [11]. In addition to pre-operative imaging, intra-operative monitoring using ultrasound or MRI thermometry may be employed to enhance the accuracy of fiber positioning and to assess thermal distribution in real time [12]. The modeling and simulation of bubble formation presented in this study are built upon these detection frameworks and aim to improve intra-procedural visualization and treatment precision by offering insights into thermal dynamics at the tissue level [13].

Numerous factors determine how laser energy affects biological tissue, including the laser's wavelength, power output, and irradiance duration, in addition to the physical and optical characteristics of the breast tissue [14]. The thermal process begins when clinicians insert a laser applicator directly into the breast cancer tumor. These applicators are often internally water-cooled, which helps dissipate excess heat and allows for deeper and more controlled energy deposition into the target tissue allowing for precise and localized thermal ablation of abnormal areas [15]. This method is minimally invasive and can be used in delicate regions such as the breast, brain or liver [16]. One major advantage of LITT technique over other ablation systems is the possibility of performing applicator placements under CT guidance while executing the actual ablation under MRI [17]. This hybrid approach enhances procedural precision and minimizes risks. Furthermore, low levels of patient radiation exposure compared to prolonged CT-guided ablation are considered a benefit when MRI is used during treatment [18]. Importantly, MR thermometry enables real-time monitoring of temperature distribution, allowing clinicians to optimize energy delivery and avoid damage to surrounding healthy tissue [19]. The compatibility with Magnetic Resonance Imaging (MRI) for real-time monitoring and control is a significant advantage of LITT Additionally, since LITT is MRI-guided, patients avoid exposure to ionizing radiation, which contrasts with conventional thermal ablation procedures that often require CT guidance. This makes LITT particularly suitable for patients requiring repeat treatments or those sensitive to radiation exposure [20-21].

Laser-induced interstitial thermotherapy (LITT) uses laser light to destroy tissue by heating it [22, 23]. This photo thermal effect happens when tissue molecules absorb the laser's light, converting it to heat. The resulting temperature increases damages cells and tissue. How the heat spreads depend on the tissue's properties and the laser's settings [24]. The extent of the damage is determined by factors like temperature, tissue properties, and heating duration. Cell death occurs through processes like apoptosis and necrosis when temperatures reach around 60°C, causing protein denaturation. While the targeted

tissue coagulates quickly, surrounding tissue experiences hyperthermia (42°–60°C), leading to further, delayed damage [25-27]. Early laser treatments focused on surface applications, but LITT allows for direct energy delivery to tumors, minimizing harm to healthy tissue. Physicians use Laser Interstitial Thermal Therapy (LITT) as a minimally invasive procedure by making either small incisions or burr holes, which significantly reduces surgical trauma, recovery time, and post-operative complications compared to traditional craniotomies or open resections. LITT delivers focused laser energy directly to the tumor site via optical fibers, enabling highly localized ablation. This contrasts with earlier laser treatments that were limited to superficial tissues, often causing unintended damage to nearby healthy structures. A major advantage of LITT is the integration with MRI systems that enable real-time monitoring of thermal dose and lesion formation. This MRI thermometry allows clinicians to manage ablation zone precisely, reducing risk of damaging surrounding breast regions. LITT avoids the use of ionizing radiation, unlike CT-guided procedures or traditional radiotherapy. This benefit is especially important for patients requiring multiple treatments, younger individuals, or those with radiation sensitivity. LITT is well-suited for treating tumors in eloquent or surgically challenging areas of the breast. This procedure acts as medical treatment for individuals who cannot benefit from traditional open surgery. due to the tumor's location or the patient's health condition. The minimally invasive character of LITT enables patients to enjoy both quicker hospital release periods and quicker recovery times in comparison to conventional surgical methods. LITT can be safely repeated and used alongside other treatment modalities such as chemotherapy, targeted therapy, or stereotactic radiosurgery. It can also be combined with a biopsy in a single session, improving diagnostic and therapeutic efficiency [20, 21]. However, early LITT lacked real-time imaging and treatment planning, which limited its effectiveness. During LITT procedures water acts as the main component because it maintains superior laser energy absorption capabilities and transforms this energy into thermal energy. The water content and procedure temperature measurements in LITT treatment were recorded by Yang et al. [28-31] as early as 2007. The main laser energy absorption process in LITT procedures occurs through water due to its specific property. When the laser activates its emission of focused light at precise wavelengths water molecules in targeted tissue absorb this energy better than the rest of tissue contents [32, 33].

The purpose of this computational model revolves around recreating heat evaporation and bubble development for LITT applications. The main purpose is investigating the detailed physical interactions between intense laser energy and biological tissue through in-depth study. The research details mechanisms are involved with vaporization while describing bubble initiation and bubble movement. A theoretical and mathematical framework is developed within this computational model for analyzing basic vaporization principles during LITT procedures.

2. Materials and Methodology

The bio-heat transfer equation establishes the fundamental explanation of how laser energy interacts with tissue through delivery. The full model takes into account a combination of tissue properties, including: specific heat capacity and thermal conductivity of tissue, perfusion rate of blood, temperature, optical properties of tissue, tissue density and parameters of laser wavelength, power and duration of laser pulse. The equation is stated as [2].

$$\rho C_p \frac{\partial T}{\partial t} - \nabla \cdot (\kappa \nabla T) + \xi_b \big(T - T_b\big) = Q_{\text{rad}} \quad \text{in } (0,\tau) \times \Omega \tag{2.1}$$

$$T(0,\cdot) = T_{\text{init}} \quad \text{in } \Omega \tag{2.2}$$

In above equation $T = T(x,t)$ represents temperature of tissue, liable on point $x \in \Omega$ over time interval $t \in (0,\tau)$. The specific heat capacity C_P, the density of the tissue ρ, and κ represents thermal conductivity. Blood perfusion rate is signified by ξ_b and temperature of blood is represented by T_b. Finally, irradiation of the laser Q_{rad} [J] depicts energy source and distribution of tissue temperature at primary point is T_{init}. The equation describes how laser light interacts with biological tissue while it absorbs energy and scatters part of the emitted energy. The model explains photo thermal conversion in tissue cells following laser light absorption which leads to tissue damage.

The simulation relies on finite element method (FEM). The model applies the diffusion approximation from transport theory to calculate light distribution and it combines bio heat equation with tissue micro perfusion to determine thermal damage extent while accounting for temperature dependent thermal and optical properties. A damage integral provides the measures of tissue damage [34,35].

MATLAB was used to employ as computer programming software which utilized numerical methods including finite element method and Runge-Kutta method to solve governing equations for ordinary differential equations (ODEs). Multiple laser parameter, tissue property and treatment protocol adjustments are handled through simulations which helped us to develop optimized treatment methods, understand bubble dynamic structures, temperature effects on tissue water density, pulse duration effects and tissue damage thresholds.

The computational research optimizes LITT treatment methods to achieve ultimate treatment outcomes while preserving nearby healthy tissue unaffected. These research findings along with results and observations are structured into this paper to benefit future professional work and research in this field.

2.1. Bubble Formation Model

LITT transmits stimulated and coherent laser energy into biological tissues containing substantial water content which leads to energy absorption because the water absorption coefficient is high in near-infrared laser wavelength ranges. Laser energy transfer into heat causes temperature elevation inside the targeted tissue regions after absorption occurs. When laser energy interacts with water molecules present inside cells it stimulates an intense temperature elevation. The constant temperature rise of water molecules eventually reaches boiling point. Cells experience a phase transition during this phase when water molecules convert from liquid to gas state thus causing water vaporization inside the cells. Vaporization happens specifically in the treated tissue where the operation takes place.Water vaporization leads to the creation of micro vapor bubbles inside the tissue. The bubbles contain steam produced through process of vaporizing water. Bubbles form and generate continuously as more water vaporizes during the process while their survival depends on tissue-specific conditions.

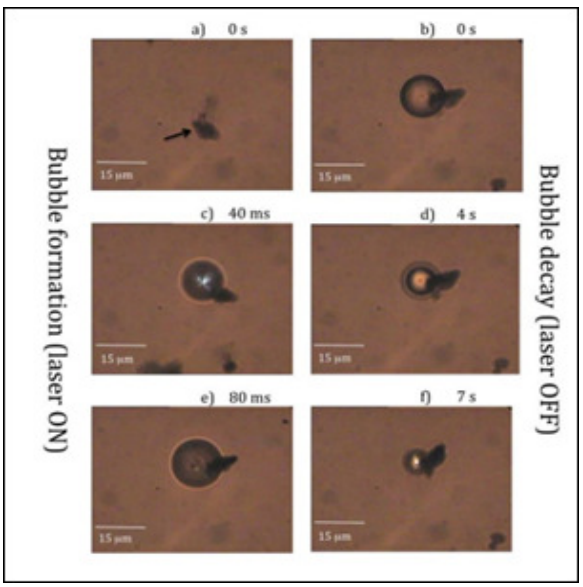

Figure 1: The temporal evolution of bubbles (left) occurs when diode laser of 1064 nm turns on at t' = 0 s followed by their degeneration (right) while laser is turned off at t" = 0 s. Laser operated with a power of 5 mW. [27].

.

Cycling process of bubbles creates mechanical forces which donate to tissue disruption through mechanical means. Tissue cellular damage results from the mechanical effects that occur during bubble cycle

formation and collapse along with laser-generated heat intensity. Cellular structures experience breakdown due to laser energy that also triggers cancer cell death by coagulative necrosis. Through its localized performance cancers cells can be destroyed precisely but healthy adjacent tissue remains unharmed. The bubble formation model uses a hemispherical bubble shape based on experimental observations which are shown in Figure 2.

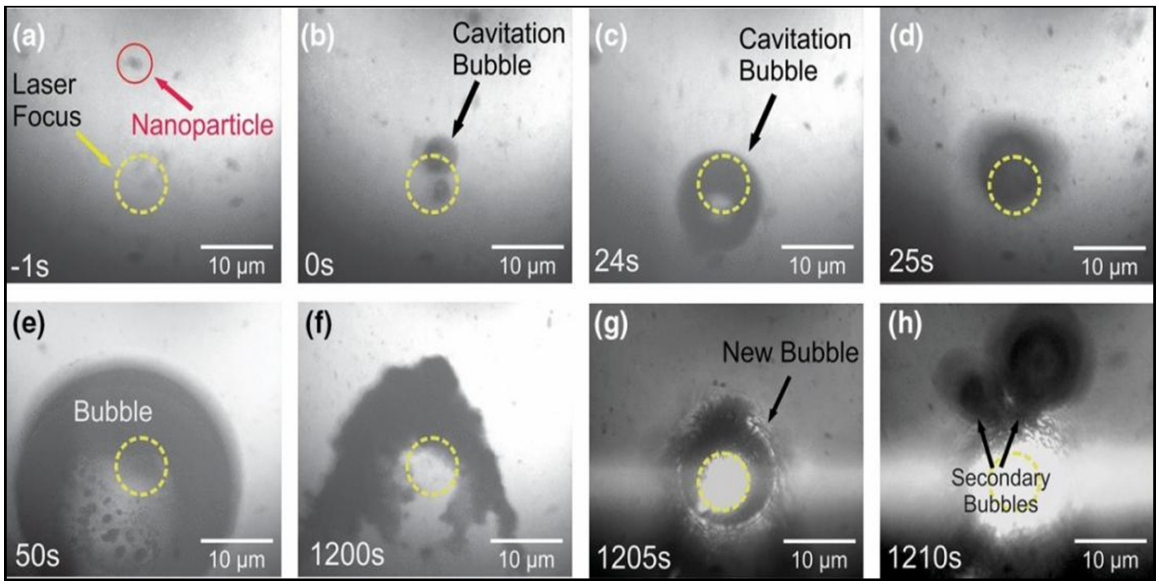

Figure 2: Formation of primary and secondary bubbles. Nanoparticle accumulation process and Laser-induced bubble formation. The times presented in the study count from when bubbles first emerged. (a) The red circular nanoparticle moves directionally toward the area where the laser emitted light concentrates (dotted circle in yellow color). (b) Air bubble is produced by Laser focus after nanoparticle enters its region. The small bubble reaches only 5 micrometers across, and it does not stay within the laser focus zone. (c) The bubble expands although it maintains its position outside the focal area. (d) The bubble achieves a position exactly within the laser focus but it simultaneously drifts beyond the focal zone of the camera device. (e) The surface of the bubble displays both nanoparticles as well as bubbles grown from the solution. (f) After the bubble detaches from laser focus the nanoparticle aggregate remains behind. (g) The aggregate settles within the new bubble that develops in the focused area. (h) Within aggregate, trapped ethanol forms extra bubbles. The use of 8 mW and 16mW for super continuum and pump pulses exists in [36].

3. Results and Discussion

3.1. Tissue Water Density

The laser energy path of LITT activates targeted tissue that triggers localized temperature elevation. The elevated temperature level produces water vaporization in tissue matter resulting in decreased density of water molecules throughout the affected tissue region. To study how temperature affects tissue water density we developed mathematical model equation-(3.1). (part-1) for temperature range 0°C to 103°C, equation-A (part-2) for temperature range 103°C to 104°C and equation-1 (part-3) for temperature range 104°C to 200°C via MATLAB. We produced a graphic that shows the derivative of water density along with temperature to examine changes in water density.

$$W(M) = 800 \cdot \begin{cases} 1 - e^{\left(\frac{M-106}{3.42}\right)} & \text{if } M \leq 103^{\circ}\text{C}, \\ R(M) & \text{if } 103^{\circ}\text{C} < M \leq 104^{\circ}\text{C}, \\ e^{\left(\frac{80-M}{34.37}\right)} & \text{if } 104^{\circ}\text{C} \leq M, \end{cases} \tag{3.1}$$

Where $R(M)$ is key that inserts among two exponential function and is assumed as:

$$R(M) = 3.713 \times 10^{-2} M^3 - 11.475 M^2 + 1.182 \times 10^3 M - 4.058 \times 10^4 \tag{3.2}$$

Water tissue density experiences changes when exposed to heat in accord with Figure 3 (a). Supply of heat at these temperatures below 100°C primarily affects tissue and water contents by raising their temperature. The tissue water vapors increase while temperature reaches 100°C causing water density to decrease progressively until most of the tissue water evaporates. The rate of water density change decreases with temperature progression until the measurement reaches 100°C according to Figure 3(b). The rate of water density adjustment sharpens at the instant temperature touches 100°C.

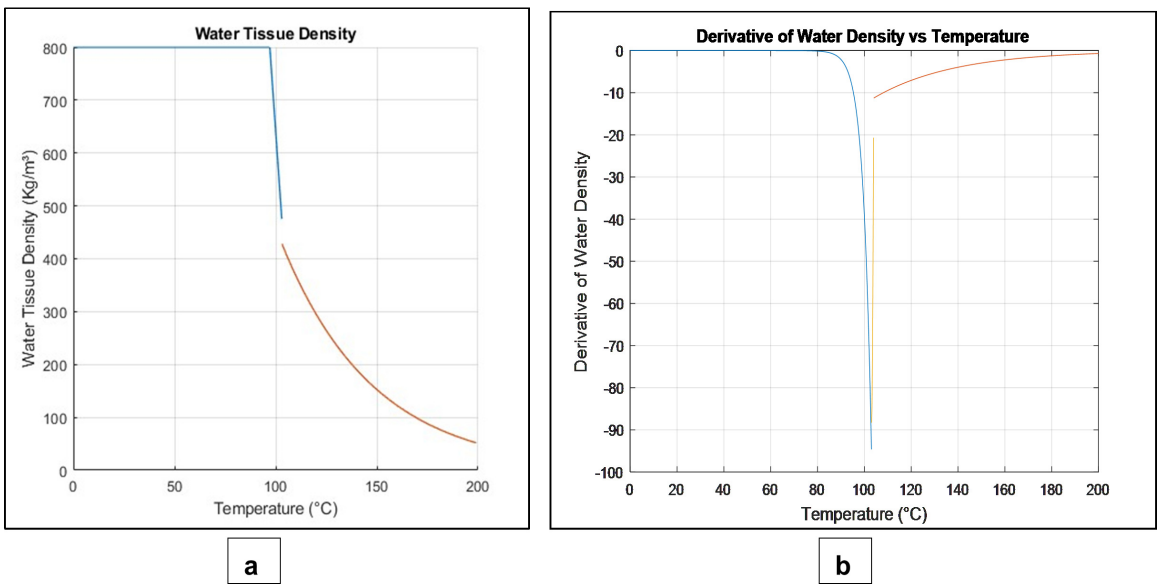

Figure 3: (a) The first graph displays the density of water through temperature variations and (b) The second depicted visual shows the derivative of water density against temperature alterations

3.2. Effect of Laser Fluence

The treatment's overall safety and efficacy increases together with healthy tissues preservation when laser fluence maintenance stands as a fundamental factor by regulating the absorption depth of light into materials. We analyzed the laser tissue effects through a relationship that connects laser fluence with absorption depth by using equation:

$$d = \frac{1}{\alpha} \ln\left(\frac{F}{F_t}\right) \tag{3.3}$$

The above equation defines α that represents absorption coefficient while F indicates Laser fluence and F_t serves as threshold fluence. Measurement of Laser fluence occurs in units of joules per square centimeter (J/cm^2)[37,38]. The effect of Laser fluence on the tissue is depicted in Figure 4. At low values of laser fluence, the absorption depth reached its peak but subsequently decreased slightly. A short duration of sufficient laser energy served to pull all cell electrons out to an infinite distance. The

electrostatic forces supersede cohesive forces due to Coulomb explosion after intense laser beams discharge multiple electrons to generate positive ions.

Loss of these electrons weakened chemical bonding and enabled Coulomb repulsion to overcome them and resulted in explosion of positive ions and electrons. The research indicates that cell damage rises as the number of low-energy laser pulses climbs but damage only occurs during the first laser pulses when energy levels become higher. No cell destruction happened as the number of pulses continued to increase during this phase. The observation finds justification through the understanding that multiple strong laser energy pulses disrupt cells while extra pulses fail to interact with surviving cells.

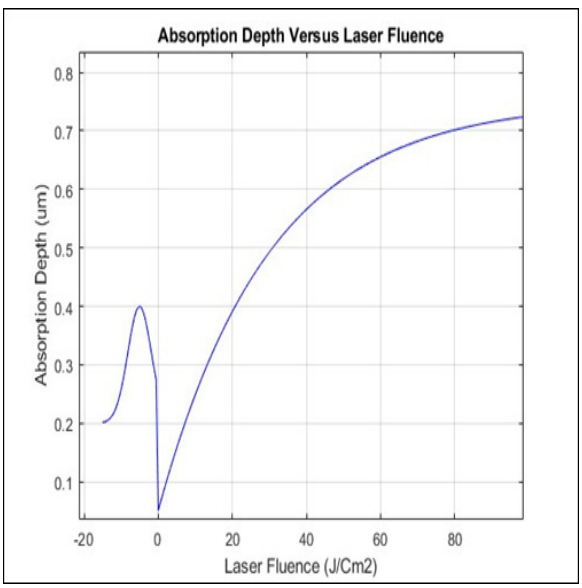

Figure 4: The graph shows how laser fluence affects absorption depth measurement

3.3. Damage Function

Tissue damage is modelled by Arrhenius Law defined as:

$$\omega_{(t,x)} = A \int_0^t A e^{-\frac{E_a}{RT}}\, ds \tag{3.4}$$

Here, damage rate constant is symbolized by $\omega_{(t,x)}$, frequency factor is denoted by A, activation energy is denoted by E_a, real gas constant is denoted by R, and T depicts temperature. The damage rate of tissue with respect to temperature is illustrated in Figure 5. Tissue damage criteria follow a temperature scale, where comfort occurs at 0°C to 40°C, irreversible cellular damage exists at 40°C to 60°C, coagulation happens at 60°C to 100°C, vaporization occurs at 100°C, and temperatures greater than 100°C produce tissue boiling, which subsequently generates cavitations from vapor bubbles. Tissue experiences increased thermal damages at these higher temperature stages.

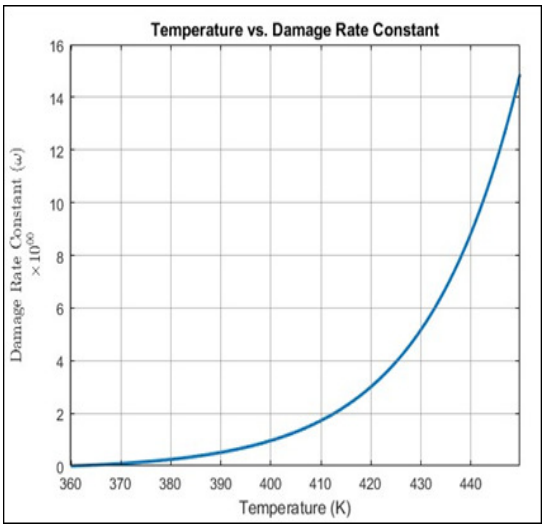

Figure 5: A Curve of Temperature and Damage Rate Constant

3.4. Size of Bubble as Function of Laser Power

The main purpose of LITT involves increasing tumor tissue temperature up to destroy it. The tissue vaporization results in bubble formation due to the water present within the tissue. Tissue bubbles develop according to the laser power averages and tissue optical characteristics per the following mathematical expression:

$$R_{\max}^3 = \left(\frac{p_i}{p_{\max}}\right)^{\frac{1}{\gamma}} \frac{\alpha}{2\pi\rho_i h}\frac{P}{f}d \tag{3.5}$$

Simulation results appear in Figure 6. A rise in laser power values at low levels caused observable enlargements in bubble size to their maximum extent. During the first phase of the plot, the slope indicated that the system responded strongly to power variations of the laser. The bubble radius growth rate slowed down because saturation limits were reached when power increased continually. Further increases in the laser power showed decreased effects on vaporization bubble dimensions according to the graph data. When laser power reaches a very high level, the relationship between additional laser power and bubble size development levels off. Additional laser power applications in this region resulted in minimal changes to the maximum bubble radius since excessive power deposited energy without enlarging the bubble size.

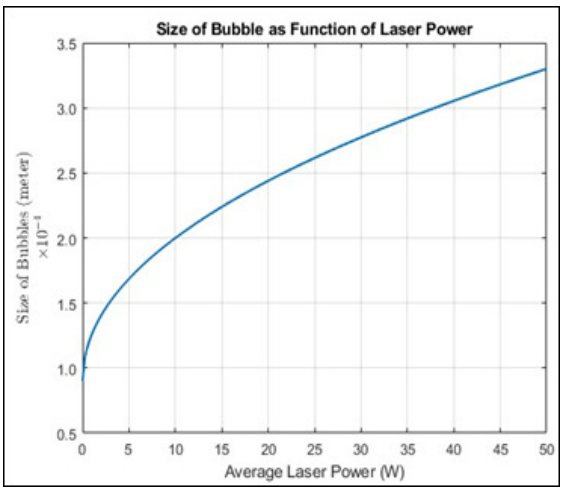

Figure 6: The size of bubbles shows direct correlation to the Average Power level of Laser (with parameters, $h = 2.84 \times 10^3\,\mathrm{J/kg}$, $\rho_i = 322\,\mathrm{kg/m^3}$, $f = 30\,\mathrm{kHz}$, $p_i = 218\,\mathrm{atm}$, absorption coefficient of water $\alpha = 100\,\mathrm{cm^{-1}}$ and $p_{\max}$ is the pressure on maximum size of bubble)

4. Conclusion

This study presented a comprehensive computational framework for analyzing bubble generation and behavior during laser-induced thermotherapy (LITT), with a specific focus on tissue vaporization. The findings underscore the critical role of water content within biological tissue, as it directly influences the formation, growing, and breakdown of vapor bubbles when exposed to high-intensity laser energy. By simulating these processes, the research captured the thermal complexities and dynamic interactions at play, offering a detailed understanding of how localized vaporization initiates and propagates. The model provided valuable insight into the thermodynamic thresholds that trigger bubble nucleation, as well as the mechanical effects these bubbles impose on surrounding tissues. Overall, this work advances the current knowledge of laser-tissue interaction by linking bubble behavior to thermal response and treatment efficacy, pave the way for more controlled and precise applications of LITT in clinical settings.

Acknowledgments

AN, SA, and AS did the writing and validation. GS, NAMZ, and RZ evaluated the technical parts and system interference.

References

1. Collaborative Group on Hormonal Factors in Breast Cancer, *Type and timing of menopausal hormone therapy and breast cancer risk: individual participant meta-analysis of the worldwide epidemiological evidence*, The Lancet, 394(10204), 1159-1168, (2019).

2. Giaquinto, A. N., Sung, H., Miller, K. D., Kramer, J. L., Newman, L. A., Minihan, A., ... & Siegel, R. L., *Breast cancer statistics, 2022*, CA: a cancer journal for clinicians, 72(6), 524-541, (2022).

3. Siegel, R. L., Miller, K. D., Fuchs, H. E., & Jemal, A., *Cancer statistics, 2022*, CA: a cancer journal for clinicians, 72(1), (2022).

4. Rami-Porta, R., & Call, S., *Sleeve lobectomy and pneumonectomy: can they really be properly compared?*, Translational Lung Cancer Research, 9(3), 434, (2020).

5. Tarver, T., *Cancer facts & figures 2012*, American cancer society (ACS) Atlanta, GA: American Cancer Society, 2012. 66 p., pdf. Available from.

6. Zhang, L., Zhu, F., Xie, L., Wang, C., Wang, J., Chen, R., ... & Zhou, M., *Clinical characteristics of COVID-19-infected cancer patients: a retrospective case study in three hospitals within Wuhan, China*, Annals of oncology, 31(7), 894-901, (2020).

7. ANSYS® Fluent®, revision 19.3.0, (2019).

8. Stat Pearls [Internet], Treasure Island (FL): Stat Pearls Publishing; 2025 Jan-Available from: https://www.ncbi.nlm.nih.gov/books/NBK430685/.

9. Lindsey, B. D., & Fuhrhop, R. W., *Laser-induced interstitial thermotherapy for breast cancer treatment: Status and future perspectives*, Journal of Surgical Oncology, 115(7), 850–858, https://doi.org/10.1002/jso.24603, (2017).

10. Blauth, S.; Hübner, F.; Leithäuser, C.; Siedow, N. & Vogl, T., *Mathematical Modeling and Simulation of Laser-Induced Thermotherapy for the Treatment of Liver Tumors*, Modeling Simulation and Optimization in the health and energy sector, 14, 3-23, (2022).

11. Saslow, D., Boetes, C., Burke, W., Harms, S., Leach, M. O., Lehman, C. D., ... & Russell, C. A., *American Cancer Society guidelines for breast screening with MRI as an adjunct to mammography*, CA: A Cancer Journal for Clinicians, 57(2), 75–89, https://doi.org/10.3322/canjclin.57.2.75, (2007).

12. Chopra, R., Colquhoun, A., Burtnyk, M., N'djin, W. A., Kobelevskiy, I., Boyes, A., & Bronskill, M. J., *MRI-controlled transurethral ultrasound therapy for conformal treatment of prostate tissue: Initial feasibility in humans*, Radiology, 246(3), 965–972, https://doi.org/10.1148/radiol.2463070364, (2008).

13. Arora, D., Qiu, J., Li, Y., & Kothapalli, S.-R., *A computational study on vapor bubble dynamics during laser-induced interstitial thermal therapy*, Journal of Biomedical Optics, 25(11), 115001, https://doi.org/10.1117/1.JBO.25.11.115001, (2020).

14. Patterson, M. S., Wilson, B. C., & Wyman, D. R., *The propagation of optical radiation in tissue I: Models of radiation transport and their application*, Lasers in Medical Science, 6(2), 155–168, https://doi.org/10.1007/BF02032591, (2001).

15. Jiang, T., Chen, H., Xu, X., Wang, C., Zuo, Z., & Fan, Y., *Interstitial laser ablation for breast cancer: A review of techniques and clinical evidence*, Frontiers in Oncology, 9, 1436, https://doi.org/10.3389/fonc.2019.01436, (2019).

16. Medvid, R., Ruiz, A., Komotar, R. J., Jagid, J., Ivan, M. E., Quencer, R. M., & Barnett, G. H., *Current applications of MRI-guided laser interstitial thermal therapy in the treatment of brain neoplasms*, Frontiers in Surgery, 2, 27, https://doi.org/10.3389/fsurg.2015.00027, (2015).

17. Kettenbach, J., Kainberger, F., Lammer, J., & Helbich, T. H., *Interstitial laser photocoagulation of breast tumors under MR guidance: Initial clinical experience*, European Radiology, 18(3), 522–529, https://doi.org/10.1007/s00330-007-0800-z, (2008).

18. Vogl, T. J., Straub, R., Eichler, K., Woitaschek, D., & Zangos, S., *Thermal ablation therapies in patients with breast cancer pulmonary metastases*, European Radiology, 22(2), 234–242, https://doi.org/10.1007/s00330-011-2257-1, (2012).

19. Kuroda, K., *Non-invasive MR thermography using the water proton chemical shift*, International Journal of Hyperthermia, 21(6), 547–560, https://doi.org/10.1080/02656730500160698, (2005).

20. Carpentier, A., McNichols, R. J., Stafford, R. J., Itzcovitz, J., Guichard, J. P., Reizine, D., Delaloge, S., Vicaut, E., Payen, D., & George, B., *Laser thermal therapy: Real-time MRI-guided and computer-controlled procedures for metastatic brain tumors*, Lasers in Surgery and Medicine, 43(10), 943–950, https://doi.org/10.1002/lsm.21139, (2011).

21. Hawasli, A. H., Bagade, S., Shimony, J. S., & Leuthardt, E. C., *Magnetic resonance imaging–guided laser interstitial thermal therapy for the treatment of gliomas*, Neurosurgery, 73(6), 1007–1017, https://doi.org/10.1227/NEU.0000000000000140, (2013).

22. Namakshenas, P., Di Matteo, F.M., Bianchi, L., Faiella, E., Stigliano, S., Quero, G., Saccomandi, P., *Optimization of laser dosimetry based on patient-specific anatomical models for the ablation of pancreatic ductal adenocarcinoma tumor*, Sci. Rep. 13, 11053, (2023).

23. Kishore, P., Kumar, S., Patel, V.M., *Conjugate heat transfer analysis of laser-irradiated cylindrical-shaped biological tissue embedded with the optical inhomogeneity*, Int. J. Heat Mass Transf. 137, 106302, (2022).

24. Partovi, B., Ahmadikia, H., Mosharaf-Dehkordi, M., *Analytical and numerical analysis of the dual-pulse lag heat transfer in a three-dimensional tissue subjected to a moving multi-point laser beam*, J. Therm. Biol. 112, 103431, (2023).

25. Hu, Y., Zhang, X.-Y., Li, X.-F., *Thermoelastic analysis of biological tissue during hyperthermia treatment for moving laser heating using fractional dual-phase-lag bioheat conduction*, Int. J. Therm. Sci. 182, 107806, (2022).

26. Mohammed, Y., Verhey, F., *A finite element method model to simulate laser interstitial thermo therapy in anatomical inhomogeneous regions*, Bio Medical Engineering, 4, 1-16, (2005).

27. George, D. S., Chidangil, S., Mathur, D., *Laser-Induced Formation of Microbubbles—Biomedical Implications*, Langmuir ACS Publications, 15, 1-45, (2018).

28. Ko, B., Lu, W., Sokolov, A. V., Lee, H. W. H., Scully, M. O., & Zhang, Z., *Multi pulse laser induced bubble formation and nanoparticle aggregation using MoS2 nanoparticles*, Scientific Reports, 10, 15753, (2020).

29. Ashiq, M. G. B., Ibrahim, N., Saeed, M. A., Shahid, M., *Laser induced Coulomb explosion of gold nanoparticles: potential role for nanophotolysis of Breast cancer*, Journal of Intense Pulsed Lasers and Applications in Advanced Physics, 2(1), 1–3, (2012).

30. Hand, D. P., *Basic Principles*, in Handbook of Laser Technology and Applications, 2nd Ed., CRC Press, Boca Raton, pp. 385-389, (2021).

31. Haley, D., Pratt, O., *Basic principles of lasers*, in Anaesthesia & Intensive Care Medicine, 18(12), 648-650, (2017).

32. Klotzkin, D. J., *Semiconductor Laser Operation*, in Introduction to Semiconductor Lasers for Optical Communications: An Applied Approach, 2nd Ed., Springer International Publishing: Cham, pp. 83-110, (2020).

33. Adamo, A. et al., *Electrically controlled white laser emission through liquid crystal/polymer multiphases*, Light: Science & Applications, 9(1), 19, (2020).

34. Banat, D., Ganguly, S., Meco, S., & Harrison, P., *Application of high-power pulsed nanosecond fibre lasers in processing ultra-thin aluminium foils*, Optics and Lasers in Engineering, 29, 106075, (2020).

35. Del Villar, I., & Matias, I. R., *Optical fibre sensors: Fundamentals for development of optimized devices*, Wiley-IEEE Press, New York, (2020).

36. Ko, B., Lu, W., Sokolov, A. V., Lee, H. W. H., Scully, M. O., & Zhang, Z., *Multi-pulse laser-induced bubble formation and nanoparticle aggregation using MoS2 nanoparticles*, Scientific Reports, 10(1), 15753, (2020).

37. Pecorino, L., *Molecular biology of cancer: Mechanisms, targets, and therapeutics*, 5th Ed., Oxford University Press, London, (2021).

38. White, F. M., Gatenby, R. A., & Fischbach, F., *The Physics of Cancer*, Cancer Research, 79(9), 2107-2110, (2019).

Asif Nawaz,
Department of Physics,
Islamia College Peshawar, KP,
Pakistan.
E-mail address: asifnawaz503@gmail.com

and

Ghulam Saddiq,
Department of Physics,
Islamia College Peshawar, KP,
Pakistan.
E-mail address: dr.saddiq@icp.edu.pk

and

Ahmad Saeed,
Department of Physics,
Federal Urdu University of Arts, Sciences and Technology, Islamabad,
Pakistan.
E-mail address: ahmad.saeed@fuuast.edu.pk

and

Rozalina Binti Zakaria,
Photonics Research Centre,
Universiti Malaya, 50603 Kuala Lumpur,
Malaysia.
E-mail address: rozalina@um.edu.my

and

N. A. Mardhiah Zainuddin,
Photonics Research Centre,
Universiti Malaya, 50603 Kuala Lumpur,
Malaysia.
E-mail address: ainaamardhiah92@gmail.com

and

Saeed Ul Islam,

Department of Mechanical Engineering,
Prince Mohammad Bin Fahd University 1664, 31952, Al Khobar,
Saudi Arabia.
E-mail address: saeedislam@awkum.edu.pk